

Formation of scalar hair on Gauss-Bonnet solitons and black holes

Yves Brihaye ^{*(1)}, Betti Hartmann ^{†(2)} and Sardor Tojiev ^{‡(2)}

⁽¹⁾Physique-Mathématique, Université de Mons-Hainaut, 7000 Mons, Belgium

⁽²⁾School of Engineering and Science, Jacobs University Bremen, 28759 Bremen, Germany

October 14, 2018

Abstract

We discuss the formation of scalar hair on Gauss-Bonnet solitons and black holes in 5-dimensional Anti-de Sitter (AdS) space-time. We present new results on the static case and point out further details. We find that the presence of the Gauss-Bonnet term has an influence on the pattern of soliton solutions for small enough values of the electric charge. We also discuss rotating Gauss-Bonnet black holes with and without scalar hair.

PACS Numbers: 04.70.-s, 04.50.Gh, 11.25.Tq

1 Introduction

Most theories of quantum gravity need more than the standard four space-time dimensions to be consistent. String theory is an example of this. The low energy effective action of these models in general reproduces Einstein gravity, but also contains terms that are higher order in the curvature invariants [1]. In five space-time dimensions this is the Gauss-Bonnet (GB) term, which has the property that the equations of motion are still second order in derivatives of the metric functions. Since black holes are thought to be the testing grounds for quantum gravity models it is of course of interest to study the generalisations of known black hole solutions to include higher order curvature corrections. As such explicit spherically symmetric and asymptotically flat black hole solutions in GB gravity are known for the uncharged case [2, 3], for the charged case [4] as well as in Anti-de Sitter (AdS) [5, 6, 7, 8] and de Sitter (dS) space-times [9], respectively. In most cases, black holes not only with spherical ($k = 1$), but also with flat ($k = 0$) and hyperbolic ($k = -1$) horizon topology have been considered. Moreover, the thermodynamics of these black holes has been studied in detail [7, 8, 10] and the question of negative entropy for certain GB black holes in dS and AdS has been discussed [6, 11].

One of the most important results of String theory is surely the AdS/CFT correspondence [12, 13] that states that a gravity theory in $(d + 1)$ -dimensional AdS space-time is equivalent to a conformal field theory (CFT) on the d -dimensional boundary of AdS. This correspondence is a weak-strong coupling duality and can be used to describe strongly coupled Quantum Field Theories on the boundary of AdS by weakly coupled gravity theories in the AdS bulk. An application of these ideas is the description of high temperature superconductivity with the help of black holes and solitons in AdS space-time [14, 15, 16, 17]. In most cases $(3 + 1)$ -dimensional solutions with planar horizons ($k = 0$) were chosen to account for the fact that high temperature superconductivity is mainly associated to 2-dimensional layers within the material. The basic idea is that at low temperatures a planar black hole in asymptotically AdS becomes unstable to the condensation of a charged scalar field since its effective mass drops below the Breitenlohner-Freedman (BF) bound [18] for sufficiently low temperature

*email: yves.brihaye@umons.ac.be

†email: b.hartmann@jacobs-university.de

‡email: s.tojiev@jacobs-university.de

of the black hole hence spontaneously breaking the $U(1)$ symmetry. It was shown that this corresponds to a conductor/superconductor phase transition. Alternatively, solitons in AdS become unstable to scalar hair formation if the value of the chemical potential is large enough. Since solitons do not have a temperature associated to them this has been interpreted as a zero temperature phase transition between an insulator and a superconductor. Interestingly, there seems to be a contradiction between the holographic superconductor approach and the Coleman-Mermin-Wagner theorem [19] which forbids spontaneous symmetry breaking in $(2+1)$ dimensions at finite temperature. Consequently, it has been suggested that higher curvature corrections and in particular GB terms should be included on the gravity side and holographic GB superconductors in $(3+1)$ dimensions have been studied [20]. However, though the critical temperature gets lowered when including GB terms, condensation cannot be suppressed – not even when backreaction of the space-time is included [21, 22, 23].

Next to the stability of solutions with flat sections and their application in the context of holographic superconductors it is of course also of interest to discuss the stability of black holes with spherical ($k = 1$) or hyperbolic ($k = -1$) horizon topology in AdS space-time.

In [24] the question of the condensation of a uncharged scalar field on uncharged black holes in $(4+1)$ dimensions has been addressed. As a toy model for the rotating case, static black holes with hyperbolic horizons ($k = -1$) were discussed. In contrast to the uncharged, static black holes with flat ($k = 0$) or spherical ($k = 1$) horizon topology hyperbolic black holes possess an extremal limit with near-horizon geometry $AdS_2 \times H^3$ [25, 26, 27]. This leads to the instability of these black holes with respect to scalar hair formation in the near-horizon geometry as soon as the scalar field mass becomes smaller than the 2-dimensional BF bound. Note that these black holes are still asymptotically AdS as long as the $(4+1)$ -dimensional BF bound is fulfilled. These studies were extended to include Gauss-Bonnet corrections [28].

In [29] static, spherically symmetric ($k = 1$) black hole and soliton solutions to Einstein-Maxwell theory coupled to a charged, massless scalar field in $(4+1)$ -dimensional global AdS space-time have been studied. The existence of solitons in global AdS was discovered in [30], where a perturbative approach was taken. In [29] it was shown that solitons can have arbitrarily large charge for large enough gauge coupling, while for small gauge coupling the solutions exhibit a spiraling behaviour towards a critical solution with finite charge and mass. The stability of Reissner-Nordström-AdS (RNAdS) solutions was also studied in this paper. It was found that for small gauge coupling RNAdS black holes are never unstable to condensation of a massless, charged scalar field, while for intermediate gauge couplings RNAdS black holes become unstable for sufficiently large charge. For large gauge coupling RNAdS black holes are unstable to formation of massless scalar hair for all values of the charge. Moreover, it was observed that for large gauge coupling and small charges the solutions exist all the way down to vanishing horizon. The limiting solutions are the soliton solutions mentioned above. On the other hand for large charge the limiting solution is a singular solution with vanishing temperature and finite entropy, which is not a regular extremal black hole [31]. These results were extended to a tachyonic scalar field as well as to the rotating case [32]. Recently, solutions in asymptotically global AdS in $(3+1)$ dimensions have been studied in [33]. It was pointed out that the solutions tend to their planar counterparts for large charges since in that case the solutions can become comparable in size to the AdS radius. The influence of the Gauss-Bonnet corrections on the instability of these solutions has been discussed in [34].

In this paper, we are interested in Gauss-Bonnet solitons as well as black holes in $(4+1)$ -dimensional AdS space-time. We study the case of solitons in more detail and point out further details in comparison to [34]. Moreover, we also discuss static and rotating Gauss-Bonnet black holes with and without scalar hair. The rotating solutions without scalar hair have been previously studied in asymptotically flat space-time [35, 36, 37] as well as in AdS space-time [38, 37]. Our paper is organized as follows: we present the model in Section 2, while we discuss solitons in Section 3. In Section 4, we present our results for the black holes and we conclude in Section 5.

2 The model

In this paper, we are studying the formation of scalar hair on electrically charged black holes and solitons in (4 + 1)-dimensional Anti-de Sitter space-time. The action reads :

$$S = \frac{1}{16\pi G} \int d^5x \sqrt{-g} \left(R - 2\Lambda + \frac{\alpha}{2} (R^{MNKL} R_{MNKL} - 4R^{MN} R_{MN} + R^2) + 16\pi G \mathcal{L}_{\text{matter}} \right), \quad (1)$$

where $\Lambda = -6/L^2$ is the cosmological constant and α is the Gauss-Bonnet coupling with $0 \leq \alpha \leq L^2/4$. $\alpha = 0$ corresponds to Einstein gravity, while $\alpha = L^2/4$ is the so-called Chern-Simons limit. $\mathcal{L}_{\text{matter}}$ denotes the matter Lagrangian which reads :

$$\mathcal{L}_{\text{matter}} = -\frac{1}{4} F_{MN} F^{MN} - (D_M \psi)^* D^M \psi - m^2 \psi^* \psi, \quad M, N = 0, 1, 2, 3, 4, \quad (2)$$

where $F_{MN} = \partial_M A_N - \partial_N A_M$ is the field strength tensor and $D_M \psi = \partial_M \psi - ie A_M \psi$ is the covariant derivative. e and m^2 denote the electric charge and mass of the scalar field ψ , respectively.

The coupled gravity and matter field equations are obtained from the variation of the action with respect to the matter and metric fields, respectively, and read

$$G_{MN} + \Lambda g_{MN} + \frac{\alpha}{2} H_{MN} = 8\pi G T_{MN}, \quad M, N = 0, 1, 2, 3, 4, \quad (3)$$

where H_{MN} is given by

$$H_{MN} = 2 (R_{MABC} R_N^{ABC} - 2R_{MANB} R^{AB} - 2R_{MA} R_N^A + R R_{MN}) - \frac{1}{2} g_{MN} (R^2 - 4R_{AB} R^{AB} + R_{ABCD} R^{ABCD}) \quad (4)$$

and T_{MN} is the energy-momentum tensor

$$T_{MN} = g_{MN} \mathcal{L}_{\text{matter}} - 2 \frac{\partial \mathcal{L}_{\text{matter}}}{\partial g^{MN}}. \quad (5)$$

In the following, we want to study rotating Gauss-Bonnet solitons and black holes in (4 + 1) dimensions. In general, such a solution would possess two independent angular momenta associated to the two independent planes of rotation. Here, we will restrict ourselves to the case where these two angular momenta are equal to each other. The Ansatz for the metric reads [39]

$$ds^2 = -b(r) dt^2 + \frac{1}{f(r)} dr^2 + g(r) d\theta^2 + h(r) \sin^2 \theta (d\varphi_1 - \omega(r) dt)^2 + h(r) \cos^2 \theta (d\varphi_2 - \omega(r) dt)^2 + (g(r) - h(r)) \sin^2 \theta \cos^2 \theta (d\varphi_1 - d\varphi_2)^2, \quad (6)$$

where θ runs from 0 to $\pi/2$, while φ_1 and φ_2 are in the range $[0, 2\pi]$. The solution possesses two rotation planes at $\theta = 0$ and $\theta = \pi/2$ and the isometry group is $\mathbb{R} \times U(2)$. In the following, we will additionally fix the residual gauge freedom by choosing $g(r) = r^2$.

For the electromagnetic field and the scalar field we choose :

$$A_M dx^M = \phi(r) dt + A(r) (\sin^2 \theta d\varphi_1 + \cos^2 \theta d\varphi_2), \quad \psi = \psi(r). \quad (7)$$

Note that originally the scalar field is complex, but that we can gauge away the non-trivial phase and choose the scalar field to be real. The coupled, non-linear ordinary differential equations depend on four independent constants: Newton's constant G , the cosmological constant Λ (or Anti-de Sitter radius L), the charge e and mass m of the scalar field. Here, we set $m^2 = -3/L^2$. The system possesses two scaling symmetries:

$$r \rightarrow \lambda r, \quad t \rightarrow \lambda t, \quad L \rightarrow \lambda L, \quad e \rightarrow e/\lambda, \quad A(r) \rightarrow \lambda A(r), \quad h(r) \rightarrow \lambda^2 h(r) \quad (8)$$

as well as

$$\phi \rightarrow \lambda \phi, \quad \psi \rightarrow \lambda \psi, \quad A(r) \rightarrow \lambda A(r), \quad e \rightarrow e/\lambda, \quad \gamma \rightarrow \gamma/\lambda^2 \quad (9)$$

which we can use to set $L = 1$ and γ to some fixed value without losing generality. In the following, we will choose $\gamma = 9/40$ unless otherwise stated.

Note that the metric on the AdS boundary in our model is that of a static 4-dimensional Einstein universe with boundary metric $\gamma_{\mu\nu}$, $\mu, \nu = 0, 1, 2, 3$ given by

$$\gamma_{\mu\nu} dx^\mu dx^\nu = -dt^2 + L^2 (d\theta^2 + \sin^2 \theta d\varphi_1^2 + \cos^2 \theta d\varphi_2^2) \quad (10)$$

and is hence non-rotating. This is different to the case of rotating and charged black holes in 4-dimensional AdS space-time, the so-called Kerr-Newman-AdS solutions [40], which possess a boundary theory with non-vanishing angular velocity

Asymptotically, the matter fields behave as follows

$$\phi(r \gg 1) = \mu + \frac{Q}{r^2} + \dots \quad , \quad A(r \gg 1) = \frac{Q_m}{r^2} + O(r^{-4}) \quad , \quad \psi(r \gg 1) = \frac{\psi_-}{r^{\lambda_-}} + \frac{\psi_+}{r^{\lambda_+}} + \dots \quad (11)$$

with

$$\lambda_{\pm} = 2 \pm \sqrt{4 + m^2 L_{eff}^2} \quad , \quad L_{eff}^2 = \frac{2\alpha}{1 - \sqrt{1 - 4\alpha/L^2}} \quad , \quad (12)$$

where Q and Q_m are related to the electric and magnetic charge of the solution, respectively. μ is a constant that within the context of the gauge/gravity duality can be interpreted as chemical potential of the boundary theory. For the rest of the paper we will choose $\psi_- = 0$. Within the AdS/CFT correspondence ψ_+ corresponds to the expectation value of the boundary operator in the dual theory.

The metric functions have the following asymptotic behaviour

$$\begin{aligned} f(r \gg 1) &= 1 + \frac{r^2}{L_{eff}^2} + \frac{f_2}{r^2} + O(r^{-4}) \quad , \quad b(r \gg 1) = 1 + \frac{r^2}{L_{eff}^2} + \frac{b_2}{r^2} + O(r^{-4}) \quad , \\ h(r \gg 1) &= r^2 + L_{eff}^2 \frac{f_2 - h_2}{r^2} + O(r^{-6}) \quad , \quad \omega(r \gg 1) = \frac{\omega_4}{r^4} + O(r^{-8}) \quad . \end{aligned} \quad (13)$$

The parameters in the asymptotic expansion can be used to determine the mass and angular momentum of the solutions. The energy E and angular momentum \bar{J} are

$$E = \frac{V_3}{8\pi G} 3M \quad \text{with} \quad M = \frac{f_2 - 4b_2}{6} \quad , \quad \bar{J} = \frac{V_3}{8\pi G} J \quad \text{with} \quad J = \omega_4 \quad . \quad (14)$$

In the following, we have constructed soliton as well as black hole solutions to the equations of motions numerically using a Newton-Raphson method with adaptive grid scheme [41].

3 Solitons

In the following, we would like to study globally regular, i.e. soliton-like solutions to the equations of motion. As was shown previously in [32] properly rotating solitons do not exist in our model. We will hence concentrate on the static case which corresponds to the limit $\omega(r) \equiv 0$, $A(r) \equiv 0$ and $g(r) = h(r) = r^2$. In the static case, it is also convenient to work with $a(r) \equiv \sqrt{b(r)/f(r)}$. For the remaining functions, we have to fix appropriate boundary conditions which read

$$f(0) = 1 \quad , \quad \phi'(0) = 0 \quad , \quad \psi'(0) = 0 \quad (15)$$

at the origin, where $\psi(0) \equiv \psi_0$ is a free parameter, and

$$a(r \rightarrow \infty) = 1 \quad , \quad \psi_- = 0 \quad (16)$$

on the conformal boundary. Note that the condition $\psi(0) = \psi_0$ can be replaced by fixing the electric charge $r^3 \phi'(r)|_{r \rightarrow \infty} = 2Q$. However, we found it more convenient to fix ψ_0 and determine the charge Q in dependence on this parameter.

Once fixing the parameters e^2 and α we can construct families of regular solutions labelled by the charge Q or by the mass M . The pattern of solutions turns out to be so involved that neither Q nor M can be used to characterize the solution uniquely. This is shown in Fig.1, where we give the charge Q as function of $a(0)$ and the mass M as function of $\psi(0)$, respectively. We observe that for small values of e^2 several disconnected branches exist. These solutions have the same values of M and Q , but differ in the values of $\psi(0)$ and $a(0)$. We can also formulate this statement differently: for a fixed value of $\psi(0)$ and $a(0)$ more than one solution exists. The different solutions are then characterized by different values of the mass M and charge Q .

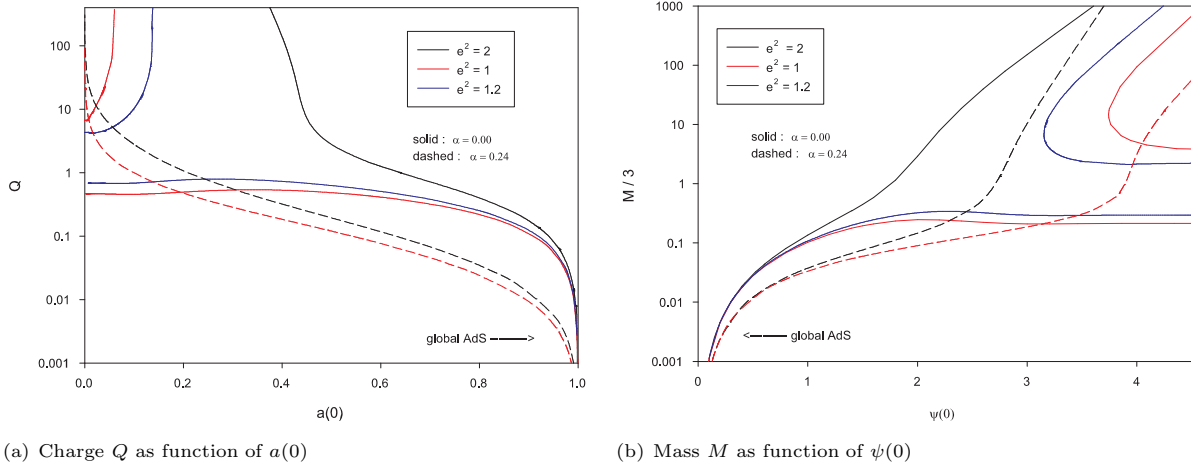


Figure 1: We show the charge Q as function of $a(0)$ (left) and the mass M as function of $\psi(0)$ (right) for three values of e^2 and two values of α . The limit corresponding to global AdS corresponds to $a(0) \rightarrow 1$ and $\psi(0) \rightarrow 0$.

As an example let us consider the case $\alpha = 0$, $e^2 = 1.2$. Here, we find that three soliton solutions exist with the same value of the scalar field at the origin $\psi(0)$. The profiles of these solutions are given in Fig. 2 (upper figure) for $\psi(0) = 3.75$. They have masses $M = 0.29$, $M = 2.15$ and $M = 418.00$, respectively. The existence of several disconnected branches had been observed before in other models [29, 33]. Here, we find that the presence of the GB term changes the general pattern in that at sufficiently large $\alpha > \alpha_{\text{cr}}$ the two branches with the lowest mass join. This is shown in Fig.3 for $\psi(0) = 3.75$ and $e^2 = 1.2$. For this choice of parameters, we find $\alpha_{\text{cr}} \approx 0.086$. For $\alpha > \alpha_{\text{cr}}$ these lowest mass solitons cease to exist. Contrary to that the solution with the highest mass can be deformed all the way to the maximal value of α , the Chern-Simons limit with $\alpha = L^2/4$. This is seen in Fig. 3.

For larger values of e^2 we find that the qualitative pattern does not change when increasing α . This is shown in Fig.4, where we give the charge Q in dependence on $a(0)$ and the mass M in dependence on $\psi(0)$ for $e^2 = 2$ and different values of α . For $\alpha = 0$ only one branch of soliton solutions exists and this persists for $\alpha \neq 0$. No new branches appear due to the presence of the GB term.

Let us mention here that the appearance of several branches is due to the presentation of data. If we would instead consider to plot asymptotically measurable quantities as e.g. the mass M , the charge Q or the free energy $F = M - \mu Q$ we would find that the solutions are uniquely described by these parameters. This is seen in Fig.5, where we give the free energy F as function of the charge Q . The plot shows that for a given value of Q there is at most ONE solution and that the free energy decreases with increasing Q . For fixed Q we find that the solution with the smallest e^2 has the lowest free energy. If we fix $\psi(0)$ as described above up to three solutions exist of which we believe the lowest mass solution to be the stable one. This solution is always on the same branch of solutions as the global AdS space-time with $M = Q = 0$.

Finally, we show the profiles of the metric and matter functions of the soliton solutions corresponding to

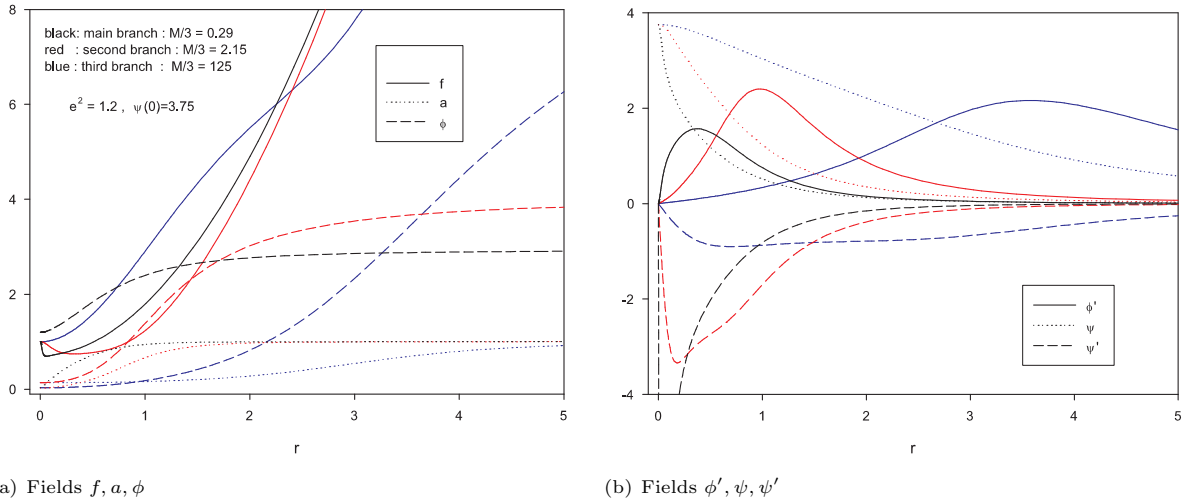


Figure 2: We show the metric functions f and a , the electric potential ϕ (left) as well as the scalar field function ψ and the derivatives ψ' and ϕ' (right) of the three different soliton solutions that exist for $\alpha = 0$, $e^2 = 1.2$ and $\psi(0) = 3.75$.

large values of α in Fig.6. The solution with $\alpha = 0.25$ corresponds to a hairy, charged Chern-Simons soliton.

4 Black holes

We are interested in solutions possessing a regular horizon at $r = r_h$. Hence we require

$$f(r_h) = 0 \quad , \quad b(r_h) = 0 \quad , \quad (17)$$

such that the metric fields have the following behaviour close to the horizon [35, 36, 37, 38]

$$\begin{aligned} f(r) &= f_1(r - r_h) + O(r - r_h)^2 \quad , \quad b(r) = b_1(r - r_h) + O(r - r_h)^2 \quad , \\ h(r) &= h_0 + O(r - r_h) \quad , \quad \omega(r) = \omega(r_h) + w_1(r - r_h) + O(r - r_h)^2 \quad , \end{aligned} \quad (18)$$

where $\omega(r_h) \equiv \Omega$ corresponds to the angular velocity at the horizon and f_1 , b_1 and h_0 are constants that have to be determined numerically. In addition there is a regularity condition for the metric fields on the horizon given by $\Gamma_1(f, b, b', h, h', \omega, \omega') = 0$, where Γ_1 is a lengthy polynomial which we do not give here. For the matter fields we have to require

$$(\phi(r) + A(r)\omega(r))|_{r=r_h} = 0 \quad , \quad \Gamma_2(\psi, \psi')|_{r=r_h} = 0 \quad , \quad (19)$$

where Γ_2 is a polynomial expression in the fields which we also do not present here.

Using the expansions of the metric functions we find that temperature T_H and the entropy S are given by [35]

$$T_H = \frac{\sqrt{f_1 b_1}}{4\pi} \quad , \quad S = \frac{V_3}{4G} r_h^2 \sqrt{h_0} \quad , \quad (20)$$

where $V_3 = 2\pi^2$ denotes the area of the three-dimensional sphere with unit radius.

4.1 Static black holes

We first study the static case with $\Omega = 0$. This has already been considered in [34]. Here we point out further important details in the pattern of solutions.

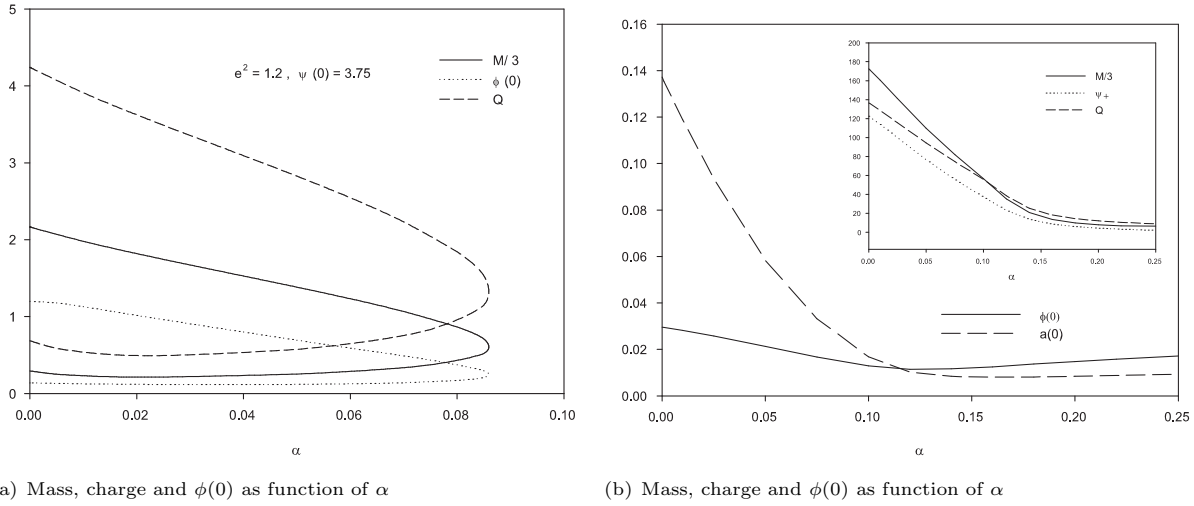


Figure 3: We show the mass M , $\phi(0)$ as well as the charge Q for the two lowest mass soliton solutions (left) as well as for the highest mass solution (right) in dependence on α . Here $\psi(0) = 3.75$ and $e^2 = 1.2$.

4.1.1 Exact solutions

In the case $\psi \equiv 0$, i.e. when the scalar field vanishes there exists an explicit solution to the equations. This reads [2, 5, 6, 7, 8]

$$f(r) = 1 + \frac{r^2}{2\alpha} \left(1 \mp \sqrt{1 - \frac{4\alpha}{L^2} + \frac{4\alpha M}{r^4} - \frac{4\alpha\gamma Q^2}{r^6}} \right), \quad a(r) = 1, \quad \phi(r) = \mu - \frac{Q}{r^2}, \quad (21)$$

where M and Q are arbitrary integration constants that can be interpreted as the mass and the charge of the solution, respectively. Note first that for $M = Q = 0$ there are two global AdS solutions with effective AdS radius $L_{\text{eff}}^2 = L^2/2 \left(1 \pm \sqrt{1 - 4\alpha/L^2} \right)$.

Since we are interested in black hole solutions here which fulfill $f(r_h) = 0$ the “+” solution is of no interest in the static case. In the limit $\alpha \rightarrow 0$, the metric function $f(r)$ of the “-” solution becomes $f(r) = 1 + \frac{r^2}{L^2} - \frac{M}{r^2} + \frac{\gamma Q^2}{r^4}$ and the corresponding solutions are Reissner-Nordström-Anti-de Sitter (RNAdS) black holes.

4.1.2 The $\alpha = 0$ limit

We first discuss the limit of vanishing Gauss-Bonnet coupling $\alpha = 0$. We find that black hole solutions exist for generic values of e^2 , r_h and $\psi(r_h)$ but that the domain of existence for these parameters is limited. It depends crucially on the value of e^2 . For large values of e^2 for which only a single branch of corresponding soliton solutions exist black holes exist for all values of $r_h > 0$ and $\psi(r_h) > 0$. In the limit $\psi(r_h) \rightarrow 0$ with r_h fixed they approach the RNAdS solution, while in the limit $r_h \rightarrow 0$ with $\psi(r_h)$ fixed they approach the corresponding soliton.

The situation is more subtle for small values of e^2 , i.e. when disconnected branches of solitons exist. This is shown in Fig. 7 for $e^2 = 1.2$, where we present the temperature and the mass of the solutions for several values of $\psi(r_h)$. We find that for sufficiently high values of $\psi(r_h)$ the black holes exist all the way down to $r_h = 0$, where they join the branch of soliton solutions. In this limit the temperature goes to infinity and the mass tends to the corresponding mass of the soliton solution. This is clearly visible for $\psi(r_h) = 3.25$ and $\psi(r_h) = 4$, respectively. On the other hand, for small values of $\psi(r_h)$ we find that the black holes exist only above a critical

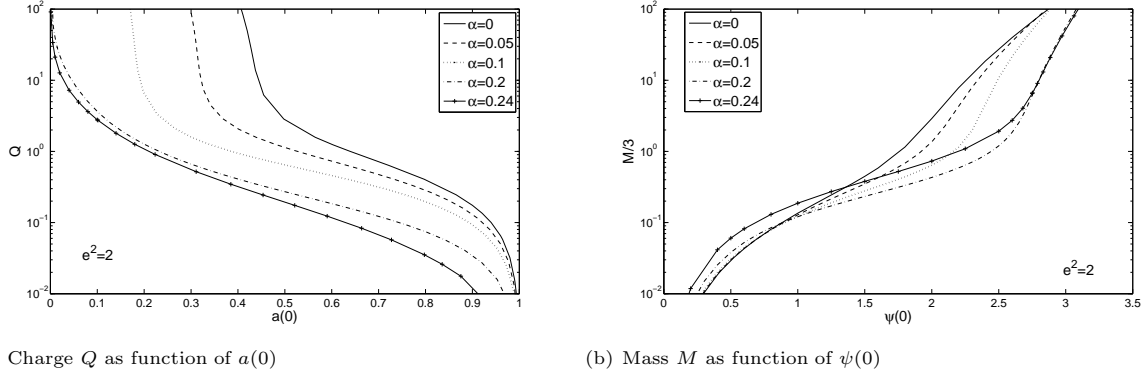


Figure 4: We show the charge Q as function of $a(0)$ (left) and the mass M as function of $\psi(0)$ (right) for soliton solutions with $e^2 = 2$ and for different values of α .

value of the horizon radius $r_h = r_h^{(cr)}$. For $r_h \rightarrow r_h^{(cr)}$ the temperature of the black hole tends to zero. However, this is not an extremal black hole, but a singular black hole solution. This is apparent when observing that $a(r_h) \rightarrow 0$ in this limit. This is clearly seen for $\psi(r_h) = 1$ and $\psi(r_h) = 2$ in Fig.7.

There should hence be a critical value of $\psi(r_h)$ at which the transition between the two pattern appears. We find that the determination of the exact numerical value of this critical $\psi(r_h)$ is quite involved, but we conjecture that it corresponds to the minimal value of $\psi(0)$ at which the disconnected branches of solitons terminate.

We further observe that if r_h is big enough (typically $r_h \gtrsim 0.5$) a connected branch of black holes with scalar hair labelled by $\psi(r_h)$ exists. This is shown in Fig. 8 for $e^2 = 1$ and $e^2 = 2$, respectively. In this figure we show the mass and temperature as function of $\psi_h \equiv \psi(r_h)$ as well as the charge as function of $a(r_h)$ of these black hole solutions. For $\psi(r_h) \rightarrow 0$, $a(r_h) \rightarrow 1$ these solutions approach the RNAdS solutions with finite values of the mass M , charge Q and temperature T_H .

4.1.3 GB black holes

In the following, we restrict our analysis to a finite number of parameters and construct mostly (unless otherwise stated) black holes with $r_h = 0.5$ and $e^2 = 1$ or $e^2 = 2$. We can then discuss the pattern of solutions for different values of α .

We find that for $\alpha \neq 0$ and for some values of the parameters e^2 and $\psi(r_h)$, the black holes can be continued up to the Chern-Simons limit $\alpha = L^2/4$. This is the case e.g. for $e^2 = 1$, $\psi(r_h) = 3.75$, $r_h = 0.5$ as shown in Fig. 9. For larger values of e^2 (with the same values of $\psi(r_h)$ and r_h) the black hole ceases to exist at some intermediate value of α where the temperature T_H tends to zero. This is shown in Fig.9 for $e^2 = 2$. To state it differently, for sufficiently large values of e^2 GB black hole solutions with scalar hair exist only up to a critical value of the GB coupling that is smaller than the Chern-Simons limit. For our specific choice of parameters here we find that solutions exist only for $\alpha \lesssim 0.14$.

4.2 Rotating black holes

In principle, we want to discuss rotating black holes with scalar hair in this paper. However, during our numerical analysis it turned out that some as yet unnoticed features appear also for rotating GB black holes without scalar hair. This is why we will discuss this case first before turning to the case with scalar hair.

4.2.1 Black holes without scalar hair

In order to understand the pattern of solutions for $\psi \equiv 0$, it is useful to recall some limiting cases. Non-rotating solutions with $\Omega = 0$ can be constructed for $\alpha \in [0, L^2/4]$, $Q \in [0, Q_m]$, where Q_m is the maximal charge up

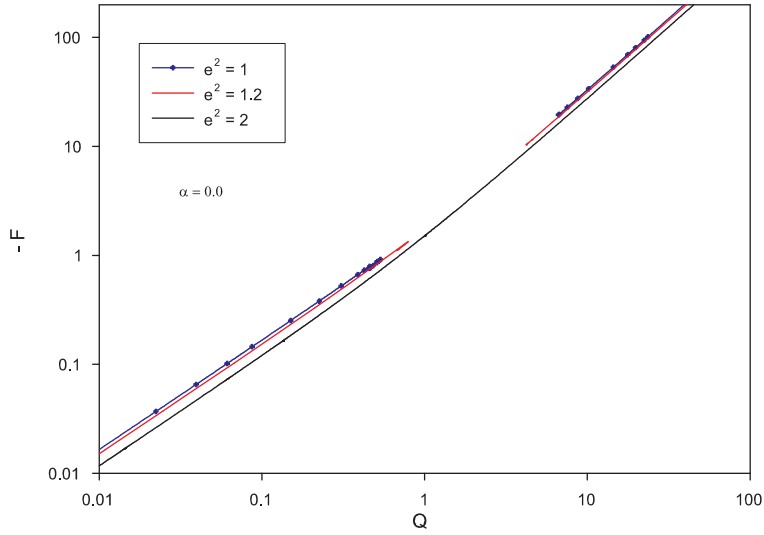


Figure 5: We show the free energy $F = M - \mu Q$ of the soliton solutions in dependence on Q for different values of e^2 and $\alpha = 0$.

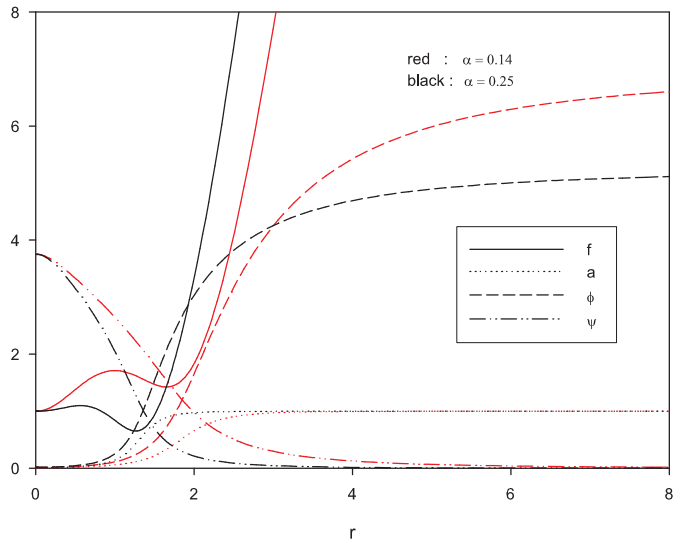


Figure 6: We show the profiles of the metric functions f and a as well as of the electric potential ϕ and the scalar field function ψ of GB solitons for two values of α and $\psi(0) = 3.75$.

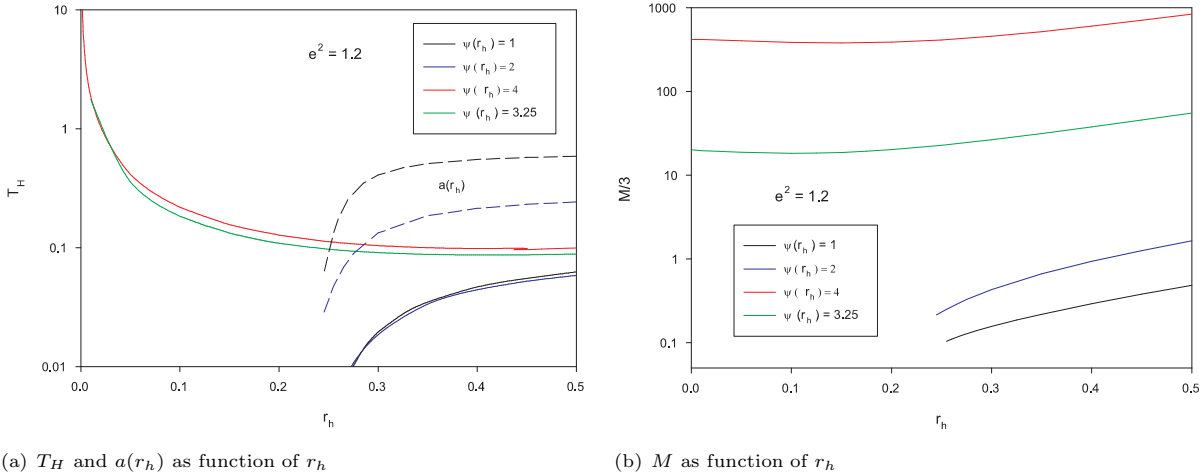


Figure 7: We show the temperature T_H , the value $a(r_h)$ (left) and the mass M (right) of black hole solutions with scalar hair for several values of $\psi(r_h)$. Here $\alpha = 0$ and $e^2 = 1.2$.

to where the solutions exist. For $\alpha = 0$ the solutions with Q fixed exist up to a maximal value of the rotation parameter $\Omega = \Omega_m$ where they become extremal [37]. For $Q = 0$ the solutions with a fixed α also exist up to a maximal value of Ω as discussed for $L^2 = \infty$ in [36] and for $L^2 < \infty$ in [37].

Let us first discuss how the solutions evolve when gradually increasing the horizon velocity Ω . Our numerical results indicate that a branch of solutions can be constructed up to a critical value $\alpha = \alpha_{cr}$ which depends on Ω such that these solutions exist for

$$0 \leq \alpha < \alpha_{cr}(\Omega) \quad , \quad \alpha_{cr}(\Omega) < \alpha_{cr}(0) = \frac{L^2}{4} \quad . \quad (22)$$

The critical value of $\alpha = \alpha_{cr}$ up to where rotating GB black holes exist depends both on Ω and Q . We find e.g. for small values of Ω , $r_h = 0.8$, $Q = 1$ that $\alpha_{cr} \approx 0.23$.

The critical phenomenon occurring in the limit $\alpha \rightarrow \alpha_{cr}$ can be understood by examining the value $h'(r_h)$. It turns out that in this limit, the value $h'(r_h)$ (which is a positive number for α large enough) increases very rapidly with α . Our numerical results further suggest that this branch cannot be continued for $\alpha > \alpha_{cr}$. This is shown in Fig.10, where the parameter $h'(r_h)$ is given as a function of α for different values of Q and Ω .

In order to understand the physical meaning of this pattern we present the temperature T_H as function of entropy S in Fig.11. This clearly shows that two branches with a transition between the branches occurring at an intermediate value of α exist. Note that small (large) entropy and large (small) temperature corresponds to α small (large). We observe that for sufficiently large α the entropy increases with increasing T_H which would signal thermodynamical stability.

Increasing the value of $h'(r_h)$ further we were able to construct a second branch of solutions for $\alpha < \alpha_{cr}$. The two branches are such that they merge at $\alpha = \alpha_{cr}$. This is shown in Fig. 12 where we present some physical quantities like the mass M and the temperature T_H in dependence on α for a rotating GB black hole solution with $\Omega = 0.02$, $Q = 1$ and $r_h = 0.8$. Although the numerical construction becomes quite involved we strongly suspect that further branches can be constructed in the region around α_{cr} . These branches, however, cannot be extended to small values of α . Surprisingly, we find that for the values of α for which the two solutions coexist the solutions of the second branch have smaller energy than the solutions on the first branch. This is demonstrated in Fig.12.

The discussion above suggests that GB black holes exist only up to a maximal value of the GB coupling. However, we know that for $\Omega = 0$ black holes also exist for all values of α up to the Chern-Simons limit $\alpha = L^2/4$.

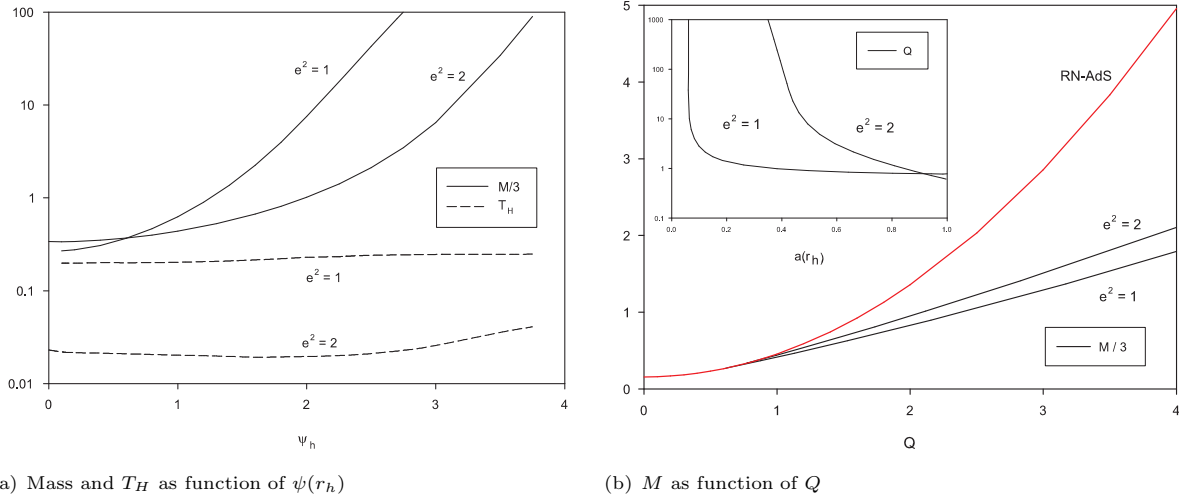


Figure 8: We show the temperature T_H and the mass M as function of $\psi_h \equiv \psi(r_h)$ (left) as well as the mass as function of charge Q for RN (red line) and hairy (black lines) black holes for two different values of e^2 (right). Here $\alpha = 0$ and $r_h = 0.5$. The charge as function of $a(r_h)$ is given in the insert.

It is therefore a natural question to attempt to construct the rotating generalizations of these solutions. We therefore considered the static solutions close to $\alpha \sim L^2/4$ and constructed rotating generalizations of these. We managed to construct another branch, i.e. a third branch of solutions in this region of the parameter. In contrast to the solutions on the other two branches, the solutions of this new branch have $h'(r_h) < 0$. In addition, we were able to construct yet another, i.e. a fourth, branch of solutions that coincides with the third one at $\alpha = \tilde{\alpha}$.

It is worth pointing out that the branches of solutions have $h'(r_h) > 0$ and $h'(r_h) < 0$, respectively. Hence they are completely disjoint. This phenomenon seems to be specific for charged, rotating solutions in asymptotically AdS. Indeed, a similar study in the case of uncharged black hole [36, 37] reveals the occurrence of a unique branch of rotating black holes.

It is also interesting to understand how these solutions behave for large rotation parameter Ω . We find that the main branch gets smoothly deformed by the rotation. The third branch becomes smaller in α and it cannot be extended continuously up to $\alpha = L^2/4$. This suggests that $\alpha = L^2/4$ is itself a critical value for rotating black holes and that charged Chern-Simons black holes cannot rotate. This, however, should be confirmed by an independent analysis which we do not aim at in this paper.

We have also studied the influence of the GB term on the solutions. We find that for small α the black hole terminates into an extremal solution at a maximal value of Ω . For larger α our numerical results suggest that several branches of solutions exist that at a critical value of Ω terminate also into an extremal solution.

4.2.2 Black holes with scalar hair

We find that rotating GB black holes with scalar hair exist for smaller values of r_h as compared to the solutions without scalar hair. Our numerical analysis of the solutions for several values of Ω and α suggests the occurrence of a phenomenon similar (although slightly more involved) to the one discussed for black holes without scalar hair. Choosing $r_h = 0.5$ and $Q = 1$ we constructed families of rotating solutions with $\alpha > 0$.

Again, the parameter $h'(r_h)$ plays a crucial role in the understanding of the pattern of solutions. This seems to diverge for (at least) four values of the parameter α , say for $\alpha = \tilde{\alpha}_k$, $k = 1, 2, 3, \dots$. By diverging we mean that it tends to $\pm\infty$ for α approaching $\tilde{\alpha}_k$ from the left and the right, respectively. This critical phenomenon seems

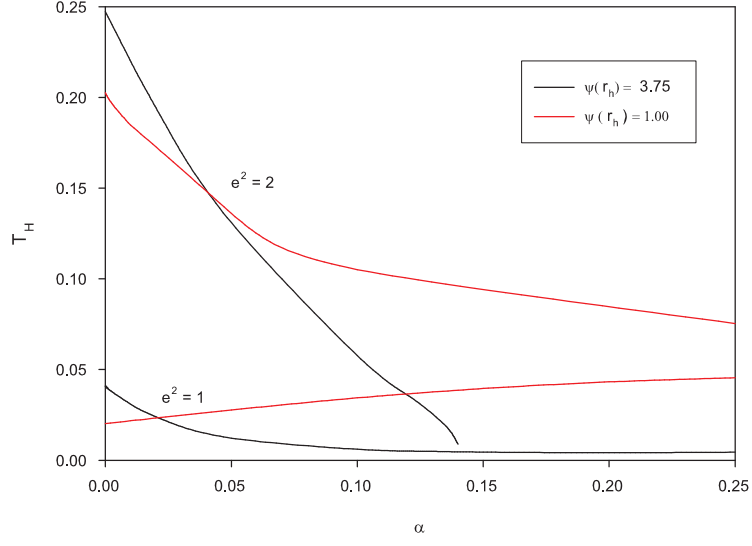


Figure 9: We show the temperature T_H of the GB black holes with scalar hair as function of α for $e^2 = 1$ and $e^2 = 2$, respectively. Here $\psi(r_h) = 3.75$ and $r_h = 0.5$.

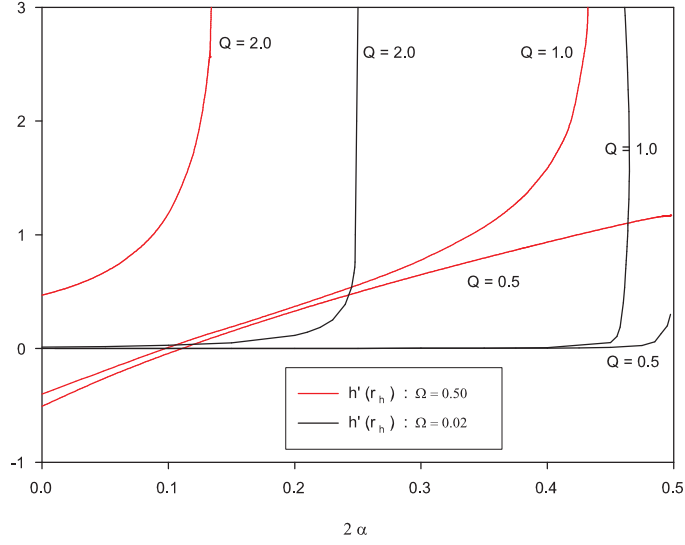


Figure 10: We show the value $h'(r_h)$ as function of α for $\Omega = 0.02, 0.5$ and $Q = 0.5, 1.0, 2.0$. Here $r_h = 0.8$, $\psi \equiv 0$.

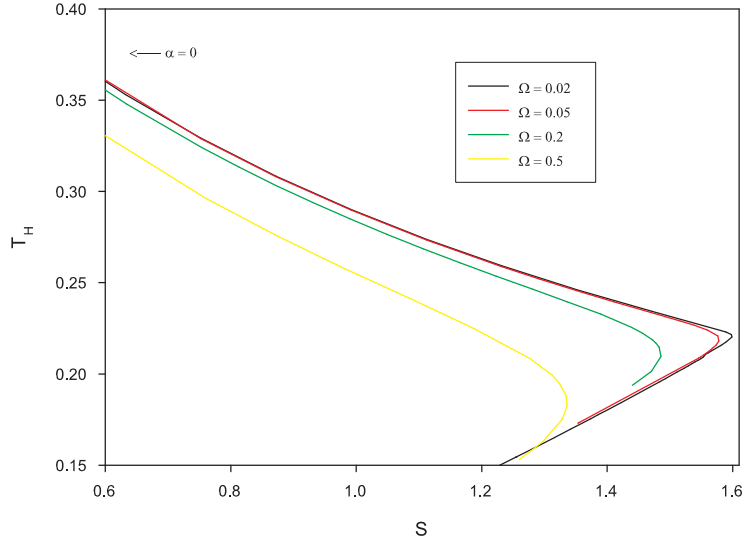


Figure 11: We show the temperature T_H as function of the entropy S for $\Omega = 0.02, 0.05, 0.2, 0.5$. Here $Q = 1$, $r_h = 0.8$ and $\psi \equiv 0$. Note that small (large) entropy and large (small) temperature corresponds to α small (large).

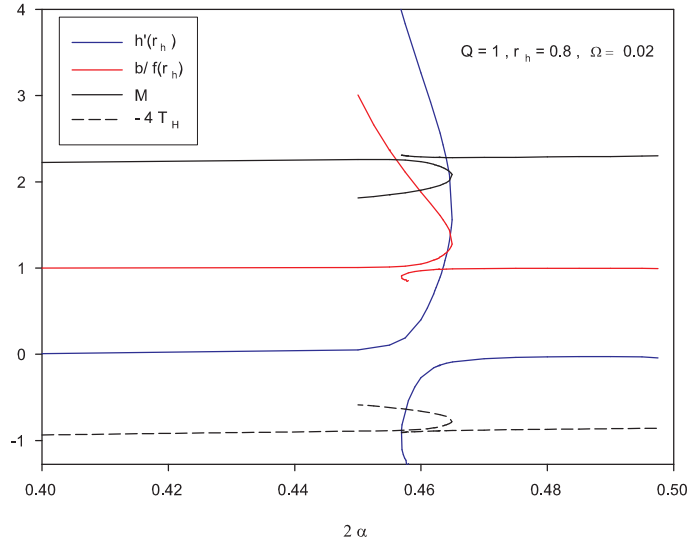


Figure 12: We show the mass M , the temperature T_H and the parameters $h'(r_h)$, $b/f(r_h)$ as functions of α for rotating GB black holes with $\Omega = 0.02$, $Q = 1$, $r_h = 0.8$ and $\psi \equiv 0$.

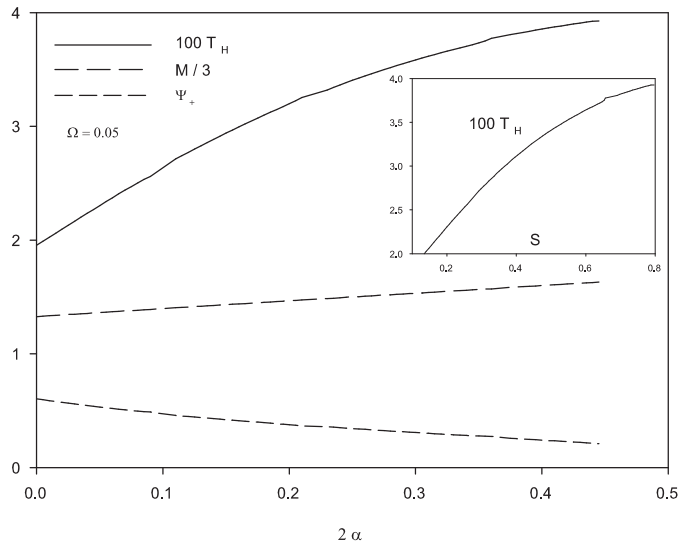


Figure 13: The mass M , temperature T_H and the value of the scalar field on the AdS boundary, ψ_+ for the rotating, hairy black holes with $Q = 1$, $r_h = 0.5$ and $\Omega = 0.05$ as function of α . We also show the temperature T_H as function of S in the subplot.

to be present already for slowly rotating black hole and persists for larger angular momentum. We observe that the critical values $\tilde{\alpha}_k$ depend only weakly on the value Ω . However, when plotting physical quantities as given in Fig. 13 we observe no discontinuities. We therefore believe that the critical values of α correspond to configurations where the coordinate gauge fixing $g(r) = r^2$ becomes accidentally not appropriate to describe the solution. Further study of this phenomenon is currently under investigation.

5 Conclusions

In this paper we have studied 5-dimensional solitons and black holes in GB gravity coupled to electromagnetic and scalar fields. In the limit of vanishing GB coupling this model reduces to Einstein-Maxwell theory coupled to a scalar field.

For vanishing scalar field the static black hole solutions are the RNAdS solution and its GB generalization. For a fixed value of the electric charge Q , these exist for horizon radius larger than a minimal value. At this minimal value the black hole becomes extremal. Black holes with scalar hair exist for smaller values of the horizon extending the domain of existence of the static black hole solutions in the r_h - Q -plane. When considering the limit $r_h \rightarrow 0$ these hairy black hole solutions tend to the corresponding soliton solutions.

In this paper, we have been mainly interested in the rotating generalizations of both types of solutions. We find that although solitons cannot be made rotating properly with non-vanishing angular momentum, the hairy black holes can be generalized to rotating solutions characterized by the angular velocity on the horizon Ω . We find that the hairy solutions can rotate up to a maximal value of Ω where we believe that they become singular. Another aspect of our study has been to investigate the effect of the GB term. In the presence of a negative cosmological constant, it is known that static asymptotically AdS solutions exist for $\alpha < L^2/4$ where L denotes the AdS radius and α the GB coupling constant. The limit $\alpha = L^2/4$ corresponds to the Chern-Simons limit. Our numerical result show that some branches of soliton solutions disappear when α is large enough. For the GB black hole solutions we find that these exist for $0 \leq \alpha \leq \alpha_{cr} < L^2/4$. Moreover, for fixed non-vanishing α several rotating solutions can exist with different values of Ω but the same value of the charge Q .

It would be interesting to find analytic arguments for our numerical results. This is currently under investigation.

Acknowledgments B.H. and S.T. gratefully acknowledge support within the framework of the DFG Research Training Group 1620 *Models of gravity*. Y.B. would like to thank the Belgian F.N.R.S. for financial support.

References

- [1] B. Zwiebach, Phys. Lett. **B156** (1985) 315; R. I. Nepomechie, Phys. Rev. **D32** (1985) 3201.
- [2] D. G. Boulware, S. Deser, Phys. Rev. Lett. **55** (1985) 2656.
- [3] J. T. Wheeler, Nucl. Phys. **B268** (1986) 737.
- [4] D. L. Wiltshire, Phys. Rev. **D38** (1988) 2445.
- [5] R. -G. Cai, Phys. Rev. **D65** (2002) 084014, [arXiv:hep-th/0109133].
- [6] M. Cvetič, S. -i. Nojiri, S. D. Odintsov, Nucl. Phys. **B628** (2002) 295, [arXiv:hep-th/0112045].
- [7] Y. M. Cho, I. P. Neupane, Phys. Rev. **D66** (2002) 024044, [arXiv:hep-th/0202140].
- [8] I. P. Neupane, Phys. Rev. **D67** (2003) 061501, [arXiv:hep-th/0212092].
- [9] R. -G. Cai, Q. Guo, Phys. Rev. **D69** (2004) 104025, [arXiv:hep-th/0311020].
- [10] I. P. Neupane, Phys. Rev. **D69** (2004) 084011, [arXiv:hep-th/0302132].
- [11] T. Clunan, S. F. Ross, D. J. Smith, Class. Quant. Grav. **21** (2004) 3447, [arXiv:gr-qc/0402044].
- [12] *see e.g.* O. Aharony, S. S. Gubser, J. M. Maldacena, H. Ooguri and Y. Oz, Phys. Rept. **323** (2000) 183 [arXiv:hep-th/9905111]; E. D'Hoker and D. Z. Freedman, arXiv:hep-th/0201253; M. Benna and I. Klebanov, *Gauge-string duality and some applications* [arXiv: 0803.1315 [hep-th]].
- [13] J. Maldacena, Adv. Theo. Math. Phys. **2** (1998) 231; Int. J. Theor. Phys. **38** (1999) 1113 [arXiv:hep-th/9711200].
- [14] S. S. Gubser, Phys. Rev. D **78** (2008) 065034 [arXiv:0801.2977 [hep-th]].
- [15] S. A. Hartnoll, C. P. Herzog and G. T. Horowitz, Phys. Rev. Lett. **101** (2008) 031601 [arXiv:0803.3295 [hep-th]]; JHEP **0812** (2008) 015 [arXiv:0810.1563 [hep-th]].
- [16] G. T. Horowitz and M. M. Roberts, Phys. Rev. **D78** (2008) 126008, [arXiv:0810.1077 [hep-th]].
- [17] *for recent reviews see* C. P. Herzog, J. Phys. A **42** (2009) 343001; S. A. Hartnoll, Class. Quant. Grav. **26** (2009) 224002 [arXiv:0903.3246 [hep-th]]; G. Horowitz, *Introduction to holographic superconductors*, arXiv:1002.1722.
- [18] P. Breitenlohner and D. Z. Freedman, Annals Phys. **144** (1982) 249.
- [19] N. D. Mermin, H. Wagner, Phys. Rev. Lett. **17** (1966) 1133; S. Coleman, Commun. Math. Phys. **31** (1973) 259.
- [20] R. Gregory, S. Kanno, J. Soda, JHEP **0910** (2009) 010, [arXiv:0907.3203 [hep-th]].
- [21] Y. Brihaye, B. Hartmann, Phys. Rev. **D81** (2010) 126008, [arXiv:1003.5130 [hep-th]].
- [22] L. Barclay, R. Gregory, S. Kanno, P. Sutcliffe, JHEP **1012** (2010) 029, [arXiv:1009.1991 [hep-th]].
- [23] M. Siani, JHEP **1012** (2010) 035. [arXiv:1010.0700 [hep-th]].
- [24] O. J. C. Dias, R. Monteiro, H. S. Reall, J. E. Santos, JHEP **1011** (2010) 036, [arXiv:1007.3745 [hep-th]].
- [25] I. Robinson, Bull. Acad. Pol. Sci. Ser. Sci. Math. Astron. Phys. **7** (1959) 351.
- [26] B. Bertotti, Phys. Rev. **116** (1959) 1331.

- [27] J. M. Bardeen, G. T. Horowitz, Phys. Rev. **D60** (1999) 104030, [arXiv:hep-th/9905099].
- [28] Y. Brihaye and B. Hartmann, Phys. Rev. D **84** (2011) 084008 [arXiv:1107.3384 [gr-qc]].
- [29] O. Dias, P. Figueras, S. Minwalla, P. Mitra, R. Monteiro, J. Santos, JHEP **1208** (2012) 117 [arXiv:1112.4447 [hep-th]].
- [30] P. Basu, J. He, A. Mukherjee and H. H. Shieh, JHEP **0911**, 070 (2009) [arXiv:0810.3970 [hep-th]].
- [31] J. Fernandez-Gracia and B. Fiol, JHEP **0911** (2009) 054 [arXiv:0906.2353 [hep-th]].
- [32] Y. Brihaye and B. Hartmann, JHEP **1203** (2012) 050 [arXiv:1112.6315 [hep-th]].
- [33] S. A. Gentle, M. Rangamani and B. Withers, JHEP **1205** (2012) 106 [arXiv:1112.3979 [hep-th]].
- [34] Y. Brihaye and B. Hartmann, Phys. Rev. D **85** (2012) 124024 [arXiv:1203.3109 [gr-qc]].
- [35] Y. Brihaye and E. Radu, Phys. Lett. B **661** (2008) 167 [arXiv:0801.1021 [hep-th]].
- [36] Y. Brihaye, B. Kleihaus, J. Kunz and E. Radu, JHEP **1011** (2010) 098 [arXiv:1010.0860 [hep-th]].
- [37] Y. Brihaye, *Charged, rotating black holes in Einstein-Gauss-Bonnet gravity*, arXiv:1108.2779 [gr-qc].
- [38] Y. Brihaye and E. Radu, JHEP **0809** (2008) 006 [arXiv:0806.1396 [gr-qc]].
- [39] J. Kunz, F. Navarro-Lerida and A. K. Petersen, Phys. Lett. B **614** (2005) 104 [gr-qc/0503010].
- [40] B. Carter, Commun. Math. Phys. **10** (1968) 280.
- [41] U. Ascher, J. Christiansen and R. D. Russell, Math. Comput. **33** (1979), 659; ACM Trans. Math. Softw. **7** (1981), 209.